

## 2D-finite element analyses and histomorphology of lag screws with and without a biconcave washer

P. Schuller-Götzburg<sup>a,b,\*</sup>, Ch. Krenkel<sup>b</sup>, T.J. Reiter<sup>c</sup>, H. Plenk Jr.<sup>a</sup>

<sup>a</sup>*Bone- and Biomaterials Research Laboratory, Histological–Embryological Institute, University of Vienna, LKA-Salzburg, Austria*

<sup>b</sup>*Department of Oral- and Maxillofacial Surgery, LKA-Salzburg, Austria*

<sup>c</sup>*Institute of Lightweight Structures and Aerospace Engineering, Vienna Technical University, Austria*

Received in final form 15 October 1998

### Abstract

For osteosynthesis and for bone transplant fixation in particular, a lag screw with a biconcave washer, the so called “Anchor Screw” (AS) has been introduced in maxillo-facial surgery. Using 2D-finite element analysis (FEA), the v.Mises and the circumferential stresses induced in underlying bone by this AS are analysed and compared to those under a conventional lag screw. The stress distributions below the biconcave washer of the AS were correlated with histomorphological bone reactions after AS osteosynthesis in two tumor patients, retrieved 12 weeks and 19 months after tumor surgery, respectively. Depending on the thickness of cortical bone, the v.Mises stress concentrations below the biconcave washer were lower than under the head of the conventional lag screw (CLS), but with a higher stress maximum concentrated around the rim of the washer. The circumferential stresses were only half as high around the AS, and thus the deformation of bone was reduced. As predicted by FEA, histology showed microcrack formation, but then after minimal resorption, remodelling of bone below the biconcave washer. Stable osteosynthesis could be demonstrated by bony union already after 12 weeks, and, while bone remodelling continued in the healed osteotomy, it had decreased around the screws after 19 months. It can be concluded from the biomechanical principles and the histomorphological findings that the AS appears superior to the CLS. © 1999 Elsevier Science Ltd. All rights reserved.

*Keywords:* Lag screw osteosynthesis; 2D-FE-analyses; Histomorphology

### 1. Introduction

Lag screws are well-known and clinically accepted alternatives to bone plates for achieving stable osteosynthesis or bone transplant fixation (Danis, 1949; Niederdellmann and Akuamo-Boateng, 1978; Niederdellmann and Shetty, 1987; Petzel, 1982). The underlying principle is that the lag screw glides in one bone fragment which is thus united and compressed with the other fragment when the screw is tightened.

As pointed out by Krenkel (1988, 1992), the major drawback of the conventional lag screw (CLS) is the limitation to larger angles of insertion, since the spherical CLS-head acts as a wedge with a lateral moment of force

(Ellis and Ghali, 1991) when it is inserted into the surface of cortical bone at a too small an angle. Thus, the head is pushed out of the axial orientation of the screw, which may either bend the screw or, due to stress concentration under the head and along the axis, break out a cortical fragment, before adequate interfragmentary pressure is achieved. Hence, a CLS can only be used in cases of oblique fracture or osteotomy lines, where it can be placed almost perpendicular to the cortical surface. However, in the mandible, transverse or nearly transverse fracture or osteotomy lines are much more common and would require insertion of the lag screw oblique to the cortical surface. These limitations of CLS applicability, particularly in maxillo-facial surgery, prompted Krenkel and Lixl (1988) to develop the “biconcave washer”. Together with the lag screw, it serves as an anchor and hence came to be known as the “Anchor Screw” (AS) (Kallela et al., 1995; Krenkel, 1992, 1994; Silvennoinen et al., 1995).

\* Corresponding author. Present address: Bone- and Biomaterials Research Laboratory, Histological–Embryological Institute, University of Vienna, LKA-Salzburg, Austria.

To the authors knowledge, the reaction of bone to osteosynthesis screws and their biomechanics have only been studied in connection with bone plates (Petzel, 1982; Rittmann and Perren, 1974). However, in osteosynthesis plates the head of the screw is never in direct contact with the bone, as is the case in lag screw osteosynthesis. Favourable clinical results have been obtained with the AS (Enislidis et al., 1997; Kallela et al., 1995; Knoll, 1991; Krenkel, 1992, 1994; Krenkel and Lixl, 1988; Leindekker, 1991; Silvennoinen et al., 1995), but biomechanical analyses of the stress distributions in the bone around the biconcave washer have so far been limited to optical stress analyses (Kuttner, 1989).

Therefore, in the present study the stress distributions around the biconcave washer of the AS were evaluated by 2D-finite element analysis (FEA) (Bathe, 1982; Carter and Hayes, 1977; Hughes, 1987; Huiskes and Chao, 1983), and compared to those around the CLS. In these models, the von Mises comparative stresses were calculated, so as to predict stress distributions and total stress in bone and, consequently, the bone remodelling. Secondly, the circumferential stresses and the deformation of bone were calculated, permitting the prediction of microcrack propagation. Furthermore, the *in vivo* bone reactions to AS osteosynthesis, as observed in histomorphologic evaluations of specimens retrieved from human patients, could be compared with the results of FEA.

## 2. Methods and materials

### 2.1. Finite element analysis

Both, the CLS and the AS were modelled according to the dimensions and material characteristics used for the Salzburg Titanium-Lag Screw-System® (Leibinger-GmbH, Freiburg, Germany): Screwhead diameter 4.0 mm, shaft diameter 2.0 mm, thread core 1.3 mm. Biconcave washer: outer diameter 4.0 mm, curvature radius of the spherical concavity 2.0 mm. Young's modulus  $E = 105\,000\text{ N mm}^{-2}$  for c.p. titanium.

The FE-models consisted of a bone cylinder with a central screw, inserted perpendicularly to the bone surface. This permits easy creation of the model, and the comparison of the AS with the CLS which should only be inserted nearly at right angles to the bone surface. The bone cylinder was modelled with an outer compact layer and underlying cancellous bone. Three thicknesses of the compacta (model 1 = 0.9 mm, model 2 = 1.8 mm, model 3 = 2.7 mm), and two depths of screwhead/washer insertion (model 1 = 0.3 mm, models 2 and 3 = 0.9 mm) were chosen to mimic anatomical situations. According to the literature (Rice et al., 1988), bone was assumed to be a linear elastic, isotropic material with Young's modulus  $E = 20\,000\text{ N mm}^{-2}$  for compact bone, and

$E = 1\,000\text{ N mm}^{-2}$  for cancellous bone. The Poisson's ratio was 0.35 for all materials involved.

Three axisymmetric models with the different thicknesses of the cortical layer, made up of 1200 standard isoparametric 2D-finite elements (1150 linear elements, and 50 non-linear contact elements), were used to calculate stress distributions in the bone around the lag screws, with and without biconcave washer. The FE-models were created by using the preprocessor software program PATRAN (PDA Engineering, PATRAN Division, Costa Mesa CA, USA). The FE-program ABAQUS (Hibbitt, Karlsson & Sorensen Inc., Pawtucket RI, USA) was used to perform the non-linear analyses.

The following boundary conditions were prescribed: The lateral surface of the model is assumed to be immovable in radial direction, but free to move axially. The inner surface could move only radially, while the outer cortical surface was allowed to deform freely. The interfaces between screw, washer, and surrounding bone are represented by frictionless contact, i.e. only compressive stresses normal to the interfaces can be transmitted, and the formation of gaps is allowed.

Due to the screw-to-bone contact conditions introduced into the model the problem became a non-linear one which was solved by an incremental-iterative strategy. An initial axial tensile force of 160 N was applied at the lower end of the screw, resulting in an effective stress of about  $15\text{ N mm}^{-2}$  (Perren et al., 1969; Schuller-Götzburg, 1995) to the bottom of the bone cylinder, i.e. the "osteosynthesis gap". The fields of strains and stresses in the individual regions, as well as the gap configuration along the shaft of the screw, were calculated. Stresses are represented by von Mises effective stresses, as well as by circumferential normal stresses. The stress distributions for models 1–3 were graphically plotted, and highest stress areas ( $> 3\text{ N mm}^{-2}$ ) were quantified as a percentage of the unit cortical bone area by computer-assisted planimetry, using the program LUCIA M (Laboratory Imaging Ltd., Prague, Czech Republic).

### 2.2. Histomorphological evaluation

Specimens from two patients were available for histological examination. Both patients had undergone median splitting of the mandible because of a keratinizing squamous cell carcinoma in the floor of the mouth. The tumor was removed and the two halves of the mandible were firmly screwed together with Anchor Screws placed horizontally and crosswise. The specimens were retrieved at reoperation because of local recurrence of the tumors, the first specimen 12 weeks postoperatively from a patient who had received three AS for osteosynthesis (Fig. 2a), and the second specimen 19 months postoperatively from a patient who had received two AS (Fig. 2b).

The retrieved specimens were fixed in neutral buffered formalin, radiographed, and embedded in

methylmethacrylate. The specimen blocks were then serially cut in longitudinal direction of the screws, and the ground and polished sections were examined after Giemsa surface staining by light microscopy, together with corresponding microradiographs (Plenk, 1986).

### 3. Results

#### 3.1. Distributions of von Mises stresses

In model 1 (0.9 mm compact bone), the area of highest stresses ( $> 3 \text{ N mm}^{-2}$ ) is directly adjacent to the spherical head and along the shaft of the CLS (Fig. 1a). The stresses spread laterally mainly along the cortical surface and diminish progressively as the distance to the screwhead increases. Another area of elevated stress in the shape of a quarter circle can be seen at the transition zone between the compact and cancellous bone. For the AS (Fig. 1b), the region of highest stresses concentrates around the rim of the biconcave washer, while below its concavity only lower stresses can be seen. The lateral stress distribution in compact and cancellous bone is quite similar for both screws. For respective maximum stress values and compact bone area % of highest stresses see Table 1.

In model 2 (1.8 mm compact bone), a large square-shaped region of highest stresses was again found along the screwhead and the shaft of the CLS (not shown). For the AS, an hour-glass shaped region of highest stresses was found around the rim of the washer. In both screws, the stresses  $< 3 \text{ N mm}^{-2}$  decrease laterally as the distance to the screw increases. The respective maximum stress values are higher, but the compact bone area % with highest stresses for the AS was definitely smaller than for the CLS (Table 1).

In model 3 (2.7 mm compact bone), the region of highest stresses follows the outline of the CLS (Fig. 1c) in uniform width in compact bone, with a small peak at the endosteal surface. For the AS (Fig. 1d), the region of highest stresses is concentrated around the rim of the washer and in a small endosteal area, while below the concavity of the washer and along the screwshaft the stresses do not exceed  $3 \text{ N mm}^{-2}$ . In both screws, the stresses decrease laterally, but do not extend anymore into cancellous bone. For the respective maximum stress values and the compact bone area % with stress  $> 3 \text{ N mm}^{-2}$  see Table 1.

#### 3.2. Distributions of circumferential stresses and deformation of bone

In model 1 (0.9 mm compact bone), the region of highest circumferential tensile stresses below the CLS (Fig. 1e) is much larger than below the AS (Fig. 1f) where it is more concentrated at the endosteal surface. The

maximum tensile stress ( $+ 54 \text{ N mm}^{-2}$ ) for the AS is about a half of that below the CLS ( $+ 112 \text{ N mm}^{-2}$ ), and the respective cortical bone area % is about a quarter of that below the CLS (see Table 1). The lateral distribution of tensile stresses along the endosteal surface, and the distribution of circumferential compressive stresses is almost the same below both screws (Fig. 1e and f). However, even compressive stresses are more concentrated around the rim of the washer, the maximum value of  $-107 \text{ N mm}^{-2}$  is again one-third lower than the  $-151 \text{ N mm}^{-2}$  below the CLS. Also, the cortical bone is more deformed below the CLS (Fig. 1e) and pressed away by the screwhead, thus opening in a wider gap between the screwshaft, when compared with the AS (Fig. 1f).

Similar results were obtained in models 2 and 3 with thicker compact bone (not shown), but the differences in maximum tensile stresses and cortical bone area % between the AS and CLS were less pronounced (see Table 1). Only smaller or no regions of high tensile stresses were found below both screws, and there were wider lateral stress distributions in the cortical layer which was also the less deformed, the thicker it was.

#### 3.3. Histomorphological evaluation

In specimen 1, after 12 weeks, the crosswise inserted Anchor Screws A, B and C (Fig. 2a) had apparently stabilised the osteotomy which was partially bridged by new bone formation (Fig. 3a). Due to the oblique insertion angle of all screws, the washers were obviously anchored with only one side (about half of their circumference) in cortical bone which had reacted with periosteal bone formation (Figs. 3a, 4a, 5a). At higher magnification, the rim of the washer of screw A shows tight new bone contacts (Fig. 3b) which developed on reversal cementing lines after bone resorption. Adjacent original bone with microcracks was not yet remodelled. Below the dome of the washer and along the smooth shaft of the screw the original bone seems distant, but active new bone formation can be observed (Fig. 3a and b). Most of the threads of this screw A appeared to have lost bone contacts due to resorption. Also in screw B new bone is actively formed beyond the washer upon reversal cementing lines (Fig. 4a and b). Along the smooth shaft mainly bone resorption is visible, while active new bone formation was found in the medullary cavity (Fig. 4a), and within the screw threads (not shown). In the more tangential section through the washer of screw C the dome had continuous tight contacts with the original bone surface (Fig. 5a) which apparently had not yet been resorbed. Around the rim of the washer direct bone apposition can be seen (Fig. 5b) with foregoing resorption. In the adjacent medullary cavity repeated new lamellar bone formation had led to semicircular incremental lines (Fig. 5b). Extensive bone contacts were found in the threads of this screw C (not shown).

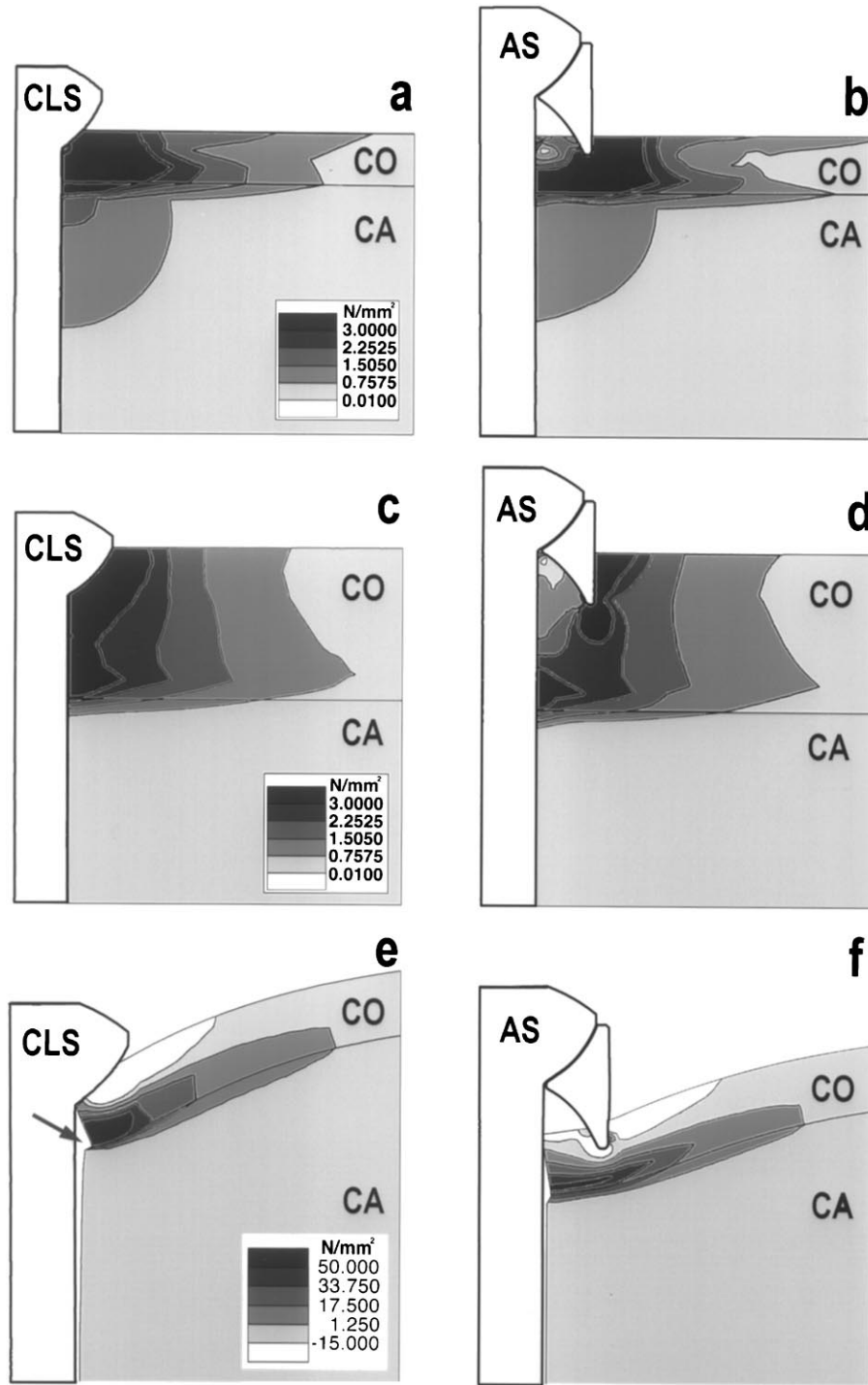


Fig. 1. (a–d) Distributions of v.Mises stresses (black area: stresses  $> 3 \text{ N mm}^{-2}$ , lower stresses in different grey tones) around the CLS and the AS. (a–b) Model 1 with 0.9 mm compact (CO) and cancellous (CA) bone. (c–d) Model 3 with 2.7 mm compact (CO) and cancellous (CA) bone. (e–f) Distributions of circumferential stresses (black area: highest tensional stresses, lower stresses in different grey tones) and deformation of bone (magn.  $\times 30$ ) below the CLS and the AS in model 1 with 0.9 mm compact (CO) and cancellous (CA) bone.

After 19 months, the osteotomy in specimen 2 had apparently healed, with restoration of the medullary cavity between cortical layers (Fig. 6). While increased vascular channels still point to ongoing remodelling around the former osteotomy gap, less remodelling and partial

incorporation can be observed in the thickened cortical bone around the washer of screw A. The threads of this screw (prototype with continuous threads) seem to have tight bone contacts. Similar tissue reactions could be observed around screw B (not shown).

Table 1  
Maximum stress values and area percentages with stresses  $>3 \text{ N mm}^{-2}$  in the 3 models of cortical bone around CLS and AS.

	CLS	AS	CLS	AS
Maximum stress				
	v.Mises stress ( $\text{N mm}^{-2}$ )		Circumferential stress ( $\text{N mm}^{-2}$ )	
Model 1	32.8	31.8	112.8	54.2
Model 2	22.9	38.6	69.1	59.6
Model 3	23.6	41.8	45.7	42.9
Area % with stresses $>3 \text{ N mm}^{-2}$				
	v.Mises stress (%)		Circumferential stresses (%)	
Model 1	19.5	20.1	4.1	0.9
Model 2	19.8	13.1	2.2	0.5
Model 3	11.3	5.8	1.5	0.4

#### 4. Discussion

In the present study, the FEA models were designed to be easily producible and reproducible, and such that the same screw with (AS) and without the washer (CLS) could be compared. However, in these models the insertion of the screws at smaller angles to the bone surface could not be calculated which would show the main advantage of the AS to the CLS. This mode of oblique insertion has already been investigated by optical stress analysis (Kuttner, 1989), and the present histomorphological observations can confirm clinical evidence of the suitability of this application (Krenkel, 1994). Owing to their symmetry, these axi-symmetric 2D models can be regarded as semi-3D models. The compact and cancellous bone tissues were assumed as isotropic materials with different E-moduli only, and the structural

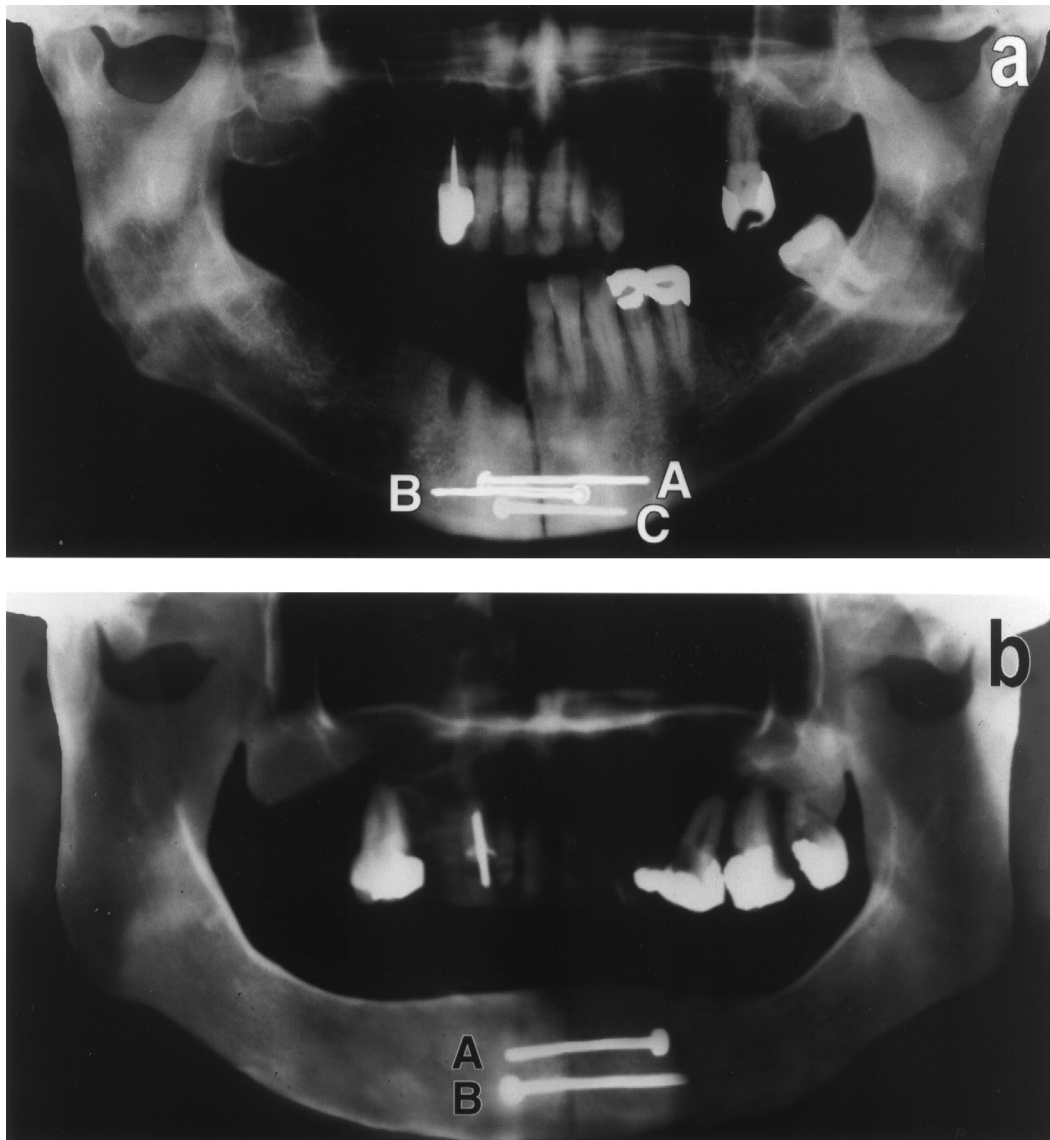


Fig. 2. (a–b) Postoperative radiographs of (a) patient 1 after osteosynthesis of the mandible with 3 Anchor Screws (A, B, C), and (b) patient 2 after osteosynthesis of the mandible with 2 Anchor Screws (A, B).

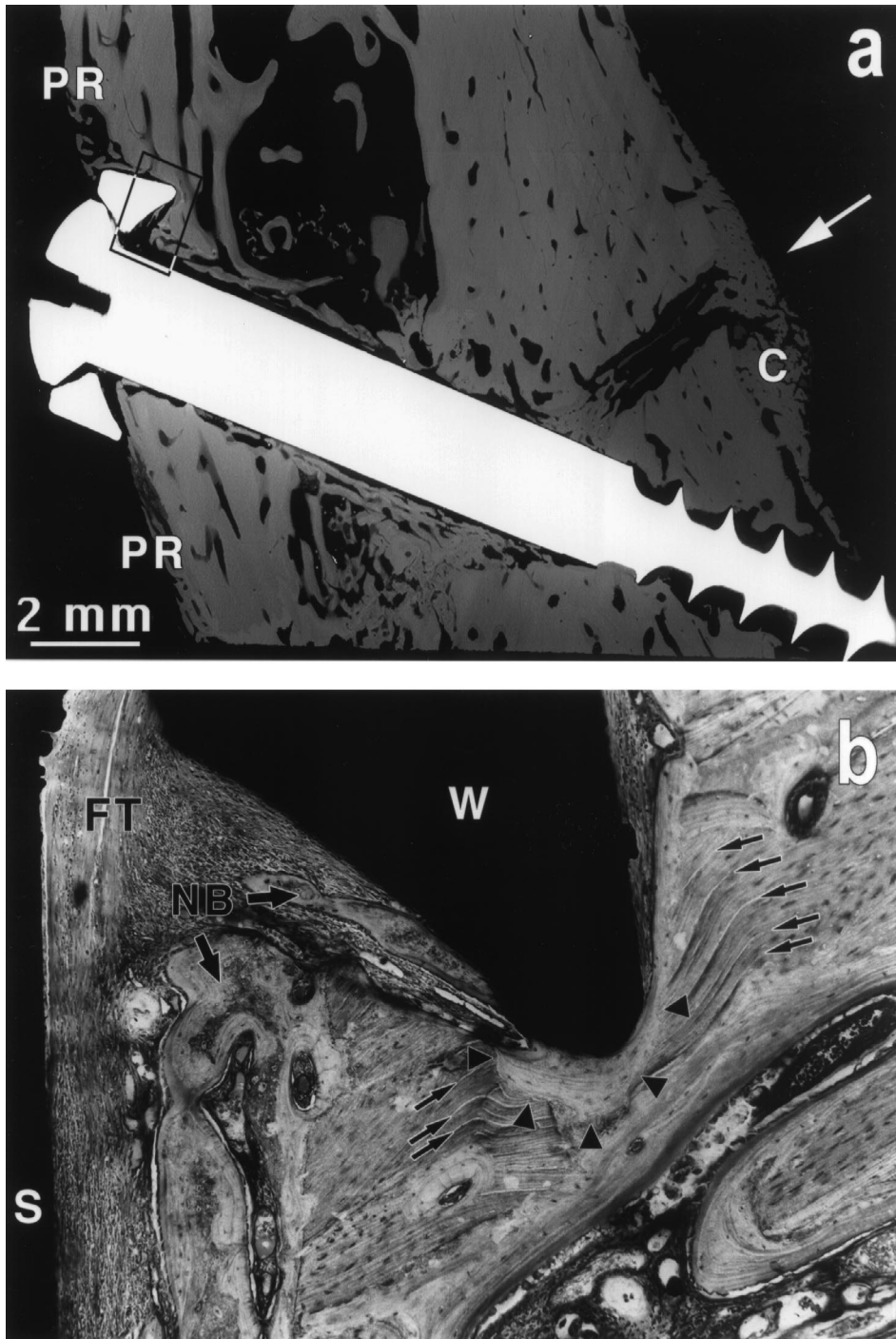


Fig. 3. (a–b) Longitudinal ground section of AS A in patient 1, retrieved 12 weeks postoperatively. (a) (Microradiograph, magn.  $10\times$ ) The screw was inserted at about  $35^\circ$  to the cortical surface, so to obtain a suitable angle to the osteotomy gap (arrow) which is partly bridged by bony callus (C). The washer appears to be anchored on only one side in the cortical bone which shows periosteal bone reactions (PR). (b) (Surface stained ground section, magn.  $85\times$ ) The enlarged detail of the rectangle in (a) shows the rim of the washer (W) in tight contact with new bone formed on a reversal cementing line (arrow heads). Microcracks (arrows) can be seen in the highly stressed original bone bed. In the fibrous tissue (FT) under the dome of the washer and along the screw shaft (S) new bone formation is visible (NB).

differences of the compact and cancellous bone were not taken into account. Also, because of the assumed isotropy of bone in these models, it did not make sense to apply the criteria proposed by Tsai-Wu (1971) for the

prediction of stress propagation and thus microcrack formation in anisotropic materials.

The von Mises stress distributions in compact bone clearly show that stresses are concentrated around the

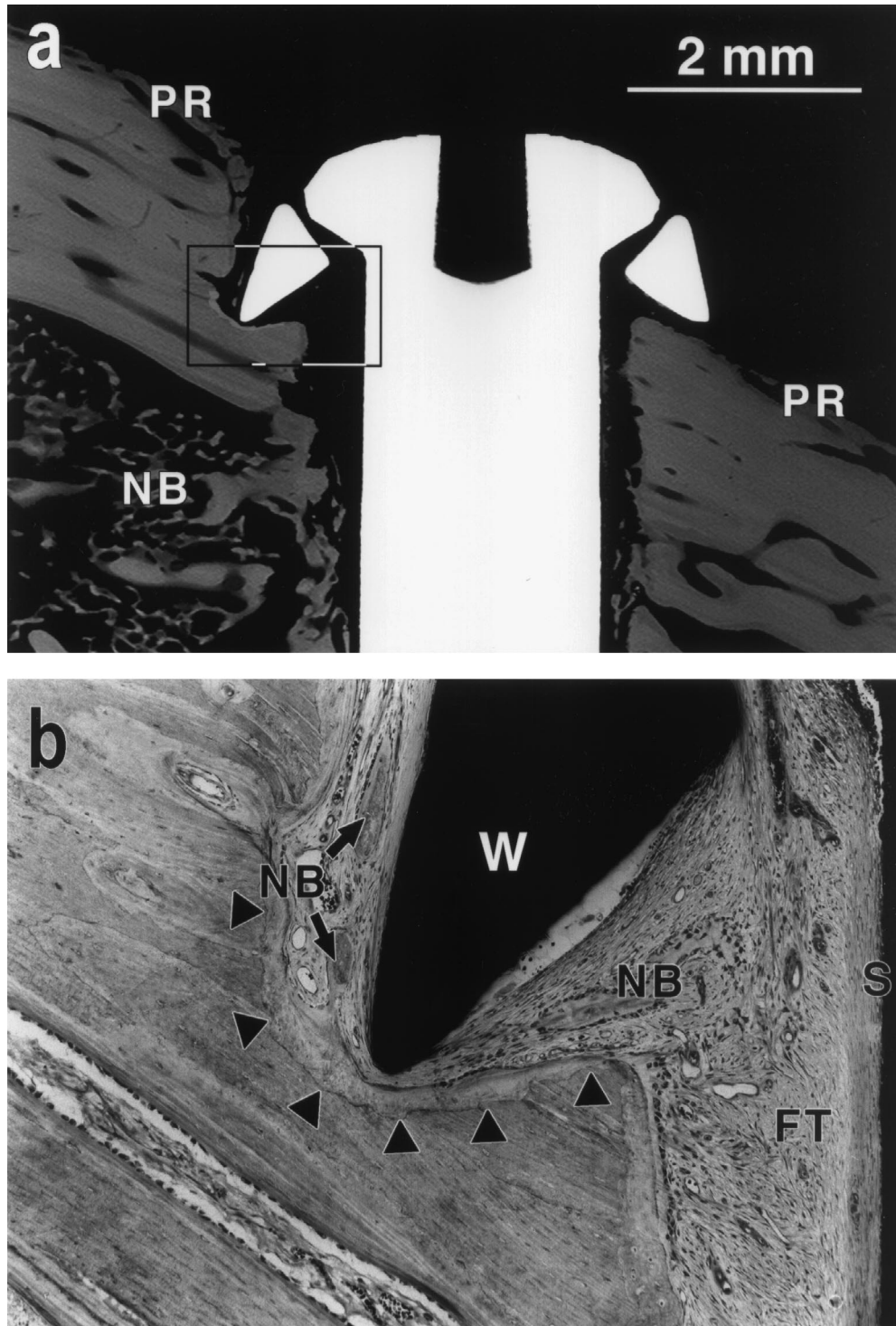


Fig. 4. (a–b) Longitudinal ground section of AS B in patient 1, retrieved 12 weeks postoperatively. (a) (Microradiograph, magn.  $20\times$ ) The screw was inserted at about  $40^\circ$  to the cortical surface which shows resorption and minimal periosteal bone reactions (PR). New bone formations (NB) mainly in the marrow cavity. (b) (Surface stained ground section, magn.  $85\times$ ) The enlarged detail of the rectangle in (a) shows the rim of the washer (W) without bone contact, but with new bone formation (NB) on a reversal cementing line (arrow heads) and in the fibrous granulation tissue (FT) under the dome and along the screw shaft (S).

rim of the biconcave washer. While the maximum stress values below the AS even increase, the regions of highest effective stresses ( $> 3 \text{ N mm}^{-2}$ ) are getting smaller, particularly below the dome of the washer, as the thickness of

compact bone increases. This subjective impression in Fig. 1a–d was substantiated by the computer-assisted planimetry of the respective compact bone area percentages. Under the head of the CLS and along the shaft

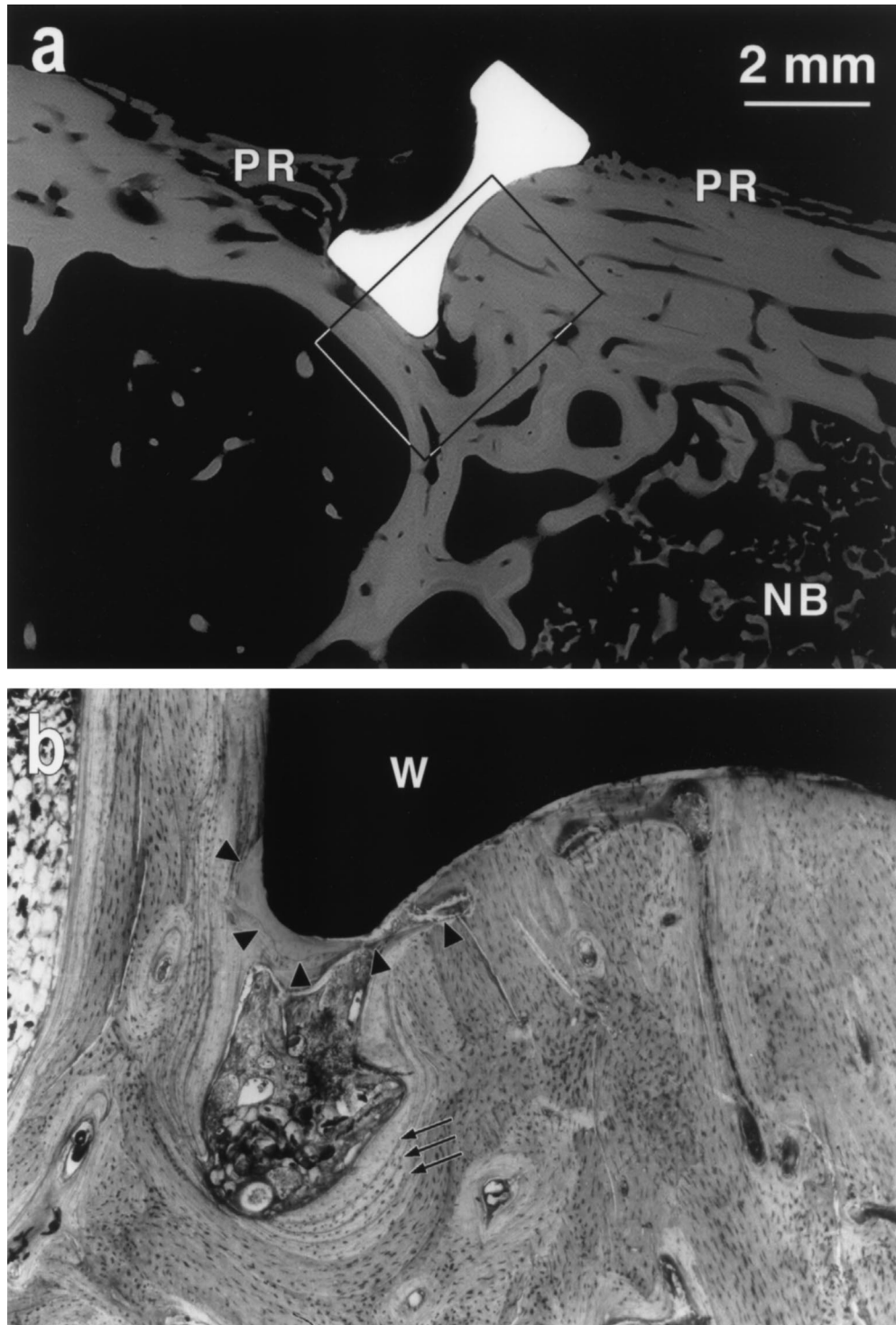


Fig. 5. (a–b) Longitudinal ground section of ASC in patient 1, retrieved 12 weeks postoperatively. (a) (Microradiograph, magn.  $10\times$ ) The tangential section of the washer shows tight passive bone contacts under the dome and around one rim, and periosteal bone reactions (PR) and new bone formation (NB) in the marrow cavity. (b) (Surface stained ground section, magn.  $70\times$ ) The enlarged detail of the rectangle in (a) shows tight contact of the rim of the washer (W) with new bone formed on a reversal cementing line (arrow heads), and then repeated new bone apposition (arrows) around a marrow space.

higher stresses were found, pointing to more deformation in bone and to the possibility of breaking out a cortical fragment, even though the oblique insertion was not tested.

Circumferential stress distributions show the advantages of the AS to be most pronounced in model 1 with thin compact bone (Fig. 1f): Compressive stresses are of course increased around the rim of the washer, and there

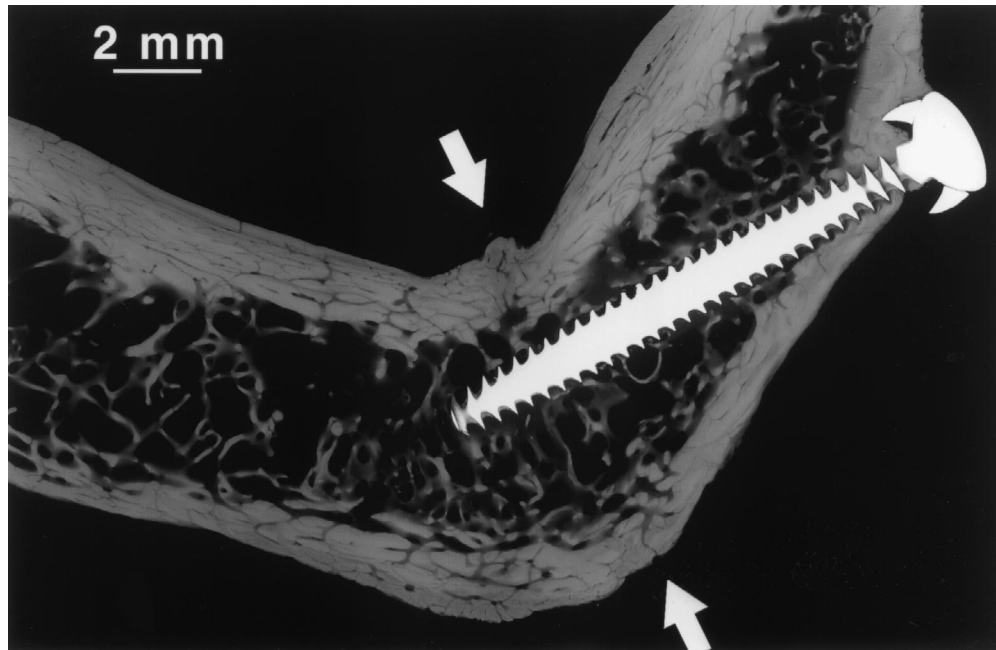


Fig. 6. Longitudinal ground section (Microradiograph, magn.  $7\times$ ) of AS A in patient 2, retrieved 19 months postoperatively. The osteotomy gap (arrows) is completely healed, and the screw and washer are incorporated in bone.

bone will be plastically deformed, or microfractures will occur, as demonstrated in our histological sections. The tensile stresses at the transition from compact to cancellous bone, however, are significantly reduced in terms of area % and maximum values ( $54$  vs.  $112 \text{ N mm}^{-2}$ ) when comparing AS and CLS (see Table 1). There is also less deformation in the cortical layer, and less gap formation along the shaft of the AS, which means less shear stresses and thus lower risk of microcrack formation.

Stress concentration as well as microfractures will cause bone necrosis, leading to resorption and consecutive bone formation (Martin and Burr, 1989). However, in lower stress areas or under stress shielding, such as below the dome of the washer and along the smooth shaft of the screw, bone resorption may not be followed by new bone formation. Both these bone reactions could be nicely demonstrated in the histomorphologic part of this study. Apparently, there was only marginal resorption of bone below the rim of the biconcave washer of the AS, followed by new bone formation. This bone reaction is in accordance with the AR(Q)F (activation, resorption, quiescence and formation) remodelling sequence described by Frost (1963) which Roberts et al. (1987) also postulated for bone implants. The foregoing resorption may first have been caused by bone damage during reaming, and then by stress concentration in this region. In fact, the shapes of the reversal cementing lines of new bone formation, as shown in Figs. 4b and 5b, do resemble the high stress fringes in the FEA model (see Fig. 1d and f). On the other hand, the microfractures around the rim of

one washer (Fig. 2b), apparently caused by too high stresses during tightening of this screw, were after 12 weeks not entirely replaced by bone remodelling which was limited to the area directly below the rim of this washer. This finding points to a time factor and local differences in the remodelling activity of bone damaged by microcracks (Martin and Burr, 1989), and thus microdamage-based criteria may be only as good as stress or strain-based criteria for the prediction of bone remodelling (Zioupos et al., 1995). If the AS is inserted obliquely, about two-thirds of the washer should be in contact with bone in the reamed groove, as postulated by Krenkel (1994). This will cause an even higher stress concentration below the rim of the washer, although this condition has not been calculated in the present FE-analysis. Maximum von Mises stress values under the rim of the biconcave washer were only calculated for perpendicular axial loading, and were not above, but rather at physiological levels reported in the literature for human cortical bone (Zioupos and Currey, 1998). Even the axi-symmetric approach chosen in the present study may thus not fully compare to the *in vivo* situation, the histological evaluation showed that the actual stress concentration under the rim of the washer did apparently not cause unlimited resorption, and consequently new bone formation could take place mainly in these former high stress regions.

On the other hand, continuous healing of the osteotomy gap (see Fig. 3a) and firm anchorage of the screw threads in bone after 12 weeks and 19 months may be regarded as evidence of stable osteosynthesis, as

described by Willenegger et al. (1971). Our results suggest that it would be appropriate to consider removal of the screws as early as three to four months after surgery, instead after the usual period of twelve months.

On the basis of the biomechanical analyses and histological findings described and discussed above it may be concluded that the AS is superior to the conventional lag screw. This combination of biconcave washer and lag screw has broadened the range of indications for this type of osteosynthesis. Clinical experiences showed (Krenkel, 1994) that the lag screw can be inserted at angles of 0–90° to the cortical surface without any risk of displacement. In cases of oblique and transverse fractures and fractures with angled wedges, the Anchor Screw can be applied orthogonal to the fracture line in keeping with the generally accepted rules of osteosynthesis (Müller et al., 1978). In addition, the present biomechanical analyses confirm that the AS offers more safety, especially in patients where the cortical layer is thin.

### Acknowledgements

This study was supported by the “Jubiläumsfonds der Österreichischen Nationalbank” (OeNB projekt no. 4729). The first author also received a scholarship from the Austrian Federal Ministry for Science and Research.

### References

- Bathe, K.J., 1982. Finite Element Procedures in Engineering Analysis. Prentice-Hall Inc., Engelwood Cliffs, NJ.
- Carter, D.R., Hayes, W.C., 1977. The compressive behavior of bone as a two-phase porous structure. *Journal of Bone and Joint Surgery* 59, 954–962.
- Danis, R., 1949. *Théorie et pratique de l'osteosynthese*. Masson, Paris.
- Ellis III, E., Ghali, G.E., 1991. Lag screw fixation of anterior mandibular fractures. *Journal of Oral and Maxillofacial Surgery* 49, 13–21.
- Enislidis, G., Pichorner, S., Wild, K., Schuller-Götzburg, P., 1997. Osteosynthesis of mandibular angle fractures with a solitary lag screw by krenkel — indications, technique and clinical results. *Stomatologie* 94, 83–90.
- Hughes, T.J.R., 1987. *The Finite Element Method: Linear Static and Dynamic Finite Element Analysis*. Prentice-Hall Inc., Engelwood Cliffs, NJ.
- Huiskes, R., Chao, E.Y.S., 1983. A survey of finite element analysis in orthopedic biomechanics: The first decade. *Journal of Biomechanics* 16, 385–409.
- Kallela, I., Söderholm, A-L., Pauku, P., Lindqvist, Ch., 1995. Lag-Screw osteosynthesis of mandibular condyle fractures: a clinical and radiological study. *Journal of Oral and Maxillofacial Surgery* 53, 1397–1404.
- Knoll, M., 1991. *Klinische Ergebnisse der Versorgung von Unterkiefercorpusfrakturen mit Ankerschrauben*. M.D. Thesis, Leopold Franzens Universität Innsbruck.
- Krenkel, Ch., 1992. Axial “anchor” screw (lag screw with biconcave washer) or “slanted-screw” plate for osteosynthesis of fractures of the mandibular condyloid process. *Journal of Cranio and Maxillofacial Surgery* 20, 348–353.
- Krenkel, Ch., 1994. *Biomechanics and Osteosynthesis of Condylar Neck Fractures of the Mandible*. Quintessenz Verlags-GmbH, Berlin.
- Krenkel, Ch., Lixl, G., 1988. Axial lag screws with doublecontoured washers. 9th Congress of the European Association for Cranio-Maxillo-Facial Surgery. Athens, Greece.
- Kuttner, P.O., 1989. *Untersuchungen zur Physikalischen Dynamik von Zug- und Tandemschrauben mit bikonkaven Unterlegscheiben am Unterkiefer*. M.D. Thesis, Leopold Franzens Universität Innsbruck.
- Leindecker, B., 1991. *Klinische Ergebnisse der Versorgung von Unterkieferkollumfrakturen mit Zugschrauben und Miniplatten*. M.D. Thesis, Leopold Franzens Universität Innsbruck.
- Martin, R.B., Burr, D.B., 1989. *Structure, Function, and Adaptation of Compact Bone*. Raven Press, New York.
- Müller, M.E., Allgöwer, M., Schneider, R., Willenegger, M., 1978. *Manual der Osteosynthese*. AO-Technik. Springer, Berlin.
- Niederdelmann, H., Akuamo-Boateng, E., 1978. Internal fixation of fractures. *International Journal of Oral Surgery* 7, 252–255.
- Niederdelmann, H., Shetty, V., 1987. Solitary lag screw osteosynthesis in the treatment of the angle of the mandible. *Plastic and Reconstruction Surgery* 82, 68–74.
- Perren, S.M., Russenberger, M., Steinemann, S., Müller, M.E., Allgöwer, M., 1969. A dynamic compression plate. *Acta Orthopaedica Scandinavica* 125, 31–41.
- Petzel, J.R., 1982. *Die Zugschraubenosteosynthese der Unterkiefer-Gelenkfortsatzfrakturen*. Biomechanik - Instrumentarium - Klinik. Habilitation an der Med. Fakultät der RWTH Aachen.
- Plenk, Jr., H., 1986. In: Williams, D.F. (Ed.), *The microscopic evaluation of hard tissue implants. Techniques of biocompatibility testing*, vol. 1. CRC Press Inc., Boca Raton, Florida, pp. 35–81.
- Rice, J.C., Cowin S.C., Bowman J.A., 1988. On the dependence of the elasticity and strength of cancellous bone on apparent density. *Journal of Biomechanics* 21, 155–168.
- Rittmann, W.W., Perren, S.M., 1974. *Corticale Knochenheilung nach Osteosynthese und Infektion*. Biomechanik und Biologie. Springer, Berlin.
- Roberts, W.E., Turley, P.K., Brezniak, N., Fielder, P.J., 1987. Bone physiology and metabolism. *Journal of California Dental Association* 15, 54–61.
- Schuller-Götzburg, P., 1995. *Die funktionsdynamische Unterkieferrekonstruktion*. Biomechanische- und histologische Untersuchungen. M.D. Thesis, University Vienna, 88.
- Silvennoinen, U., Iizuka, T., Pernu, H., Oikarinen, K., 1995. Surgical treatment of condylar process fractures using axial anchor screw fixation: a preliminary follow-up study. *Journal of Oral and Maxillofacial Surgery* 53, 884–893.
- Tsai, S.W., Wu, E.M., 1971. A General theory of strength for anisotropic materials. *Journal of Composite Materials* 5, 58–80.
- Willenegger, H., Perren, S.M., Schenk, R., 1971. Primäre und sekundäre Knochenbruchheilung. *Chirurg* 42, 241–252.
- Zioupou, P., Currey, J.D., 1998. Changes in the stiffness, strength, and toughness of human cortical bone with age. *Bone* 22, 57–66.
- Zioupou, P., Currey, J.D., Mirza, M.S., Barton, D.C., 1995. Experimentally determined microcracking around a circular hole in a flat plate of bone: comparison with predicted stresses. *Philosophical Transactions of the Royal Society of London Series. B: Biological Sciences* 347(1322), 383–396.